HHS Public Access

Author manuscript

J Med Chem. Author manuscript; available in PMC 2016 January 12.

Published in final edited form as:

J Med Chem. 2012 July 26; 55(14): 6445–6454. doi:10.1021/jm300425y.

Design, Synthesis, Calorimetry and Crystallographic analysis of 2-Alkylaminoethyl-1,1-Bisphosphonates as inhibitors of *Trypanosoma cruzi* Farnesyl Diphosphate Synthase

Srinivas Aripirala[a], **Sergio H. Szajnman**[c], **Jean Jakoncic**[b], **Juan B. Rodriguez**[c], **Roberto Docampo**[d], **Sandra B. Gabelli**[a,*], and **L. Mario Amzel**[a,*]

[a]Department of Biophysics and Biophysical Chemistry, Johns Hopkins University School of Medicine, Baltimore, Maryland 21205, USA

[b]Brookhaven National Laboratory, National Synchrotron Light Source, Upton, NY 11973

[c]Departamento de Química Orgánica and UMYMFOR (CONICET–FCEyN), Facultad de Ciencias Exactas y Naturales, Universidad de Buenos Aires, Pabellón 2, Ciudad Universitaria, C1428EHA, Buenos Aires, Argentina

[d]Center for Tropical and Global Emerging Diseases and Department of Cellular Biology, University of Georgia, Athens, Georgia 30606

Abstract

Linear 2-alkylaminoethyl-1,1-bisphosphonates are effective agents against proliferation of *Trypanosoma cruzi*--the etiologic agent of American trypanosomiasis (Chagas disease)--exhibiting IC_{50} values in the nanomolar range against the parasites. This activity is associated with inhibition at the low nanomolar level of the *T. cruzi* farnesyl diphosphate synthase (TcFPPS). X-ray structures and thermodynamic data of the complexes TcFPPS with five compounds of this family show that the inhibitors bind to the allylic site of the enzyme with their alkyl chain occupying the cavity that binds the isoprenoid chain of the substrate. The compounds bind to TcFPPS with unfavorable enthalpy compensated by a favorable entropy that results from a delicate balance between two opposing effects: the loss of conformational entropy due to freezing of single bond rotations, and the favorable burial of the hydrophobic alkyl chains. The data suggest that introduction of strategically placed double bonds and methyl branches should increase affinity substantially.

Keywords

Bisphosphonate; Trypanosoma cruzi; Chagas disease; farnesyl diphosphate synthase; FPPS; IPP; DMAPP; ITC; farnesyl pyrophosphate synthase; mevalonate pathway

[*]CORRESPONDING AUTHOR INFORMATION: L. Mario Amzel (mamzel@jhmi.edu; Ph no: 410-955-3955). Sandra B. Gabelli (gabelli@jhmi.edu; Ph no: 410-614-4146).

ACCESSION CODES

The atomic coordinates and structure factors have been deposited in the RCSB Protein Data Bank for TcFPPS+Mg^{2+} complexed with **10**+IPP (PDB code 4DWB, **11**+IPP (PDB code 4DXJ), **12**+IPP (PDB code 4DWG), **13** (PDB codes 4EIE) and **14**+IPP (PDB codes 4DZW).

INTRODUCTION

American trypanosomiasis (Chagas disease) is a major parasitic disease that affects millions of individuals world-wide[1, 2]. *T. cruzi*, the etiologic agent of American trypanosomiasis, has a complex life cycle in which it passes from a blood-sucking Reduviid insect vector to mammals.[3] It multiplies in the insect gut as an epimastigote form and is spread as a non-dividing metacyclic trypomastigote from the insect feces by contamination of intact mucosa or of wounds produced by the blood-sucking activity of the vector. In the mammalian host, the parasite proliferates intracellularly in the amastigote form and is subsequently released into the blood stream as a non-dividing trypomastigote.[3] In humans, spread of Chagas disease can also take place *via* the placenta or by blood transfusion.[4, 5] The occurrence of American trypanosomiasis in countries where the disease is not endemic has been attributed to the second mechanism.[4, 5] Chemotherapy for this neglected disease, based on old and empirically discovered drugs, is not very effective.[6] Thus, it is critical that we develop new safe drugs based on knowledge of the biochemistry and physiology of the microorganism. 2-alkylaminoethyl-1,1-bisphosphonates have emerged as a new avenue for the development of compounds active against Chagas disease.

Bisphosphonates of general formula **1** (Figure 1) are metabolically stable pyrophosphate (**2**) analogues in which a methylene group replaces the oxygen atom bridge between the two phosphorus atoms of the pyrophosphate moiety. Substitution at the carbon atom with different side chains has generated a large family of compounds.[7–10] Bisphosphonates became compounds of pharmacological importance since calcification studies were done more than 40 years ago.[11–13] Currently, several bisphosphonates (Figure 1) such as pamidronate (**3**), alendronate (**4**), risedronate (**5**), and ibandronate (**6**) are in clinical use for the treatment and prevention of osteoclast-mediated bone resorption associated with osteoporosis, Paget's disease, hypercalcemia, tumor bone metastases, and other bone diseases.

Selective action on bone is based on binding of the bisphosphonate moiety to bone mineral.[14] It has been postulated that the parasite's acidocalcisomes, organelles equivalent in composition to the bone mineral, may accumulate bisphosphonates and facilitate their antiparasitic action.[14] In the case of bone, bisphosphonates act by a mechanism that leads to osteoclast apoptosis.[15] The site of action of aminobisphosphonates has been narrowed down to the isoprenoid pathway and, more specifically, to inhibition of protein prenylation.[16] Within the isoprenoid pathway, farnesyl pyrophosphate synthase (FPPS; also called farnesyl diphosphate synthase) was identified as the main target of bisphosphonates.[17–22] FPPS catalyses two consecutive 1′-4 condensation reactions between an allylic (DMAPP or GPP) and a homoallylic substrate (IPP) to give a final product FPP. These reactions constitute the two committed steps in the biosynthesis of farnesyl pyrophosphate. In the first step it catalyzes the 1′-4 condensation of one molecule of IPP (homoallylic substrate) and one molecule of DMAPP (allylic substrate) to give GPP. In the second step it condenses one molecule of GPP and one molecule of IPP. Inhibition of the enzymatic activity of FPPS blocks farnesyl pyrophosphate and geranylgeranyl pyrophosphate formation, compounds which are required for the post-translational prenylation within osteoclasts of small GTPases such as Rab, Rho and Rac.[23]

Besides their effectiveness in long-term treatment of bone disorders, bisphosphonates exhibit a wide range of biological activities that include, in addition to stimulation of γδT cells of the immune system,[24] antibacterial,[25] herbicidal,[26] antitumor[27–30] and antiparasitic activities.[31–35]

In vivo assays showed that risedronate can significantly increase survival of *T. cruzi*-infected mice.[36] Besides being effective growth inhibitors of *T. cruzi* in *in vitro* and *in vivo* assays without toxicity to the host cells[14], bisphosphonates were found to be also effective against pathogenic trypanosomatids other than *T. cruzi*. Those include *T. brucei rhodesiense*, *Leishmania donovani*, and *L. mexicana* as well as apicomplexan parasites such as *Toxoplasma gondii* and *Plasmodium falciparum*.[33, 34, 37–43] These results point to bisphosphonates as potential candidates for chemotherapy of a range of neglected infectious diseases. They have the advantage, among other favorable characteristics, that they are relatively inexpensive and easy to synthesize. Furthermore, one may assume a low toxicity for bisphosphonate-containing drugs considering that many bisphosphonates are FDA-approved drugs that have been widely used for many years in the long-term treatment of bone disorders.

In this paper we report structural and thermodynamic studies of the interaction of five 2-alkylaminoethyl-1,1-bisphosphonates with *T. cruzi* FPPS (TcFPPS; Figure 2). The structures show that the inhibitors bind to the allylic site of the enzyme with the phosphates of the bisphosphonates coordinating three Mg^{2+} ions that bridge the compound to the enzyme in a manner similar to that observed for the physiological substrates.[44–46] The alkyl chains of the inhibitors bind within a long cavity normally occupied by the isoprenoid chain of the allylic substrate (Figure 3). The inhibitors bind to TcFPPS with high affinity despite having unfavorable enthalpy of binding. The favorable entropy that results from burying the hydrophobic alkyl chain is the main binding driving force.

Although several bisphosphonate families have been shown to inhibit the trypanosomal FPPS, the lack of pharmacokinetic studies on these compounds suggests that it is still important to expand the number of compounds in the pipeline, especially with compounds of high affinity.

The structural and thermodynamic information presented here provides the basis for the design of novel, more effective compounds for the treatment of Chagas disease. In particular, new inhibitors with strategically placed double bonds and methyl-group branches are predicted to have significantly increased affinity.

RESULTS AND DISCUSSION

Structure of the inhibitor complexes

Like the FPPS from other species, including humans, [17, 47] the farnesyl diphosphate synthase of *T. cruzi* (TcFPPS) is a physiological homodimer (monomers A and B). The structures of TcFPPS in complex with five bisphosphonates **10–14** (resolutions between 2.01 Å and 3.0 Å; Table 1) each contained, in addition, 3 divalent cations (Mg^{2+}) and isopentenyl pyrophosphate (IPP) or SO_4^{-2} (**13**-TcFPPS complex has SO_4^{-2}). Crystals of the

complexes belong to space group $P6_122$; four of the complexes have an average cell dimension of 392 Å along c-axis, 5 Å shorter than the equivalent dimension in the apo structure[48] (Table 1) indicating that the structures of the complexes pack more compactly than that of the apo enzyme.

The structures were determined by direct refinement or by molecular replacement (complex **10**-TcFPPS) using the structure of the *Trypanosoma cruzi* FPPS in complex with alendronate and IPP (1YHM). After initial refinement, 2Fo-Fc maps showed excellent density for the bound inhibitors in the region corresponding to the allylic site. In the homoallylic site, electron density for IPP is seen in four structures – **10**, **11**, **12** and **14**; in **13** a SO_4^{-2} ion occupies the homoallylic site.

In all cases, three Mg^{2+} ions bridge the phosphates of the inhibitors to the protein. The conserved aspartate residues of the two-aspartate rich motifs DDXXD (first aspartate rich motif: FARM, residues 98–102; second aspartate rich motif: SARM, residues 250–254) bind three divalent cations (Mg^{2+}) that are in turn coordinated by the phosphate backbone of the bisphosphonates (Figure 4a; **11**). The IPP is bound to the enzyme by interacting directly with arginine residues (Arg51, Arg108, and Arg360 (Figure 4b). The conserved RRG sequence (residues 107–109) of the loop following the FARM region and residues GK (263 and 264) in the loop following the SARM region are in the conformations usually seen in the closed form of the enzyme with both the allylic and homoallylic sites occupied. In all five structures the bisphosphonate, occupies the allylic site, and interacts with 3 divalent Mg^{2+} ions. Ligand waters complete the octahedral coordination of the ions.

Structural alignment of the four complexes with *n*-alkyl chains (**10–13**) shows that the phosphate backbones of the bisphosphonates interact with the same residues of the protein, located near the top of the active site (Figure 4c; Figure 5a). However, deeper into the active site there are a small number of significant differences (Figure 5b). In the **12** and **13** complexes, Tyr94 and Gln167 both move to accommodate the bisphosphonates with the longer alkyl chains. In the complex with **13**, the bisphosphonate with the longest alkyl chain, the end of the inhibitor bound to monomer A is at a distance of 3.5 Å from Ile 129 from monomer B. This additional favorable van der Waals interaction contributes to the tighter binding of **13** (Table 2) in comparison to the slightly shorter **12** (one fewer carbon).

It was proposed in earlier studies that His93 and Tyr94 (TcFPPS numbering) form the “floor” of the allylic site and determine the maximum length of the allylic substrates that can bind to the enzyme[49] and by extension the length of the inhibitors. The complexes **13**-TcFPPS and **12**-TcFPPS show that Tyr94 adopts a different conformation to accommodate longer alkyl chains (Figure 5b). Earlier studies with avian FPPS revealed that when Phe112 and Phe113 (equivalent to His93 and Tyr94 of TcFPPS) were replaced by residues with smaller side chains (Ala and Ser respectively), the mutated enzyme produced geranyl geranyl diphosphate (20 carbons)[50]. Also, in some species, geranyl geranyl diphosphate synthases contained smaller amino acids such as serine or threonine in the position equivalent to TcFPPS Tyr94 indicating that Tyr94 may be important in determining final product length[51]. These observations point to His93, Tyr94 of chain A and Ile129 of the B chain as the residues that determine maximum permissible alkyl chain length.

Comparison of the 14-TcFPPS and 10-TcFPPS complexes

In the **14**-TcFPPS structure, the cyclohexyl moiety adopts a chair conformation. Structural alignment of the **14**-TcFPPS and **10**-TcFPPS complexes shows that packing of **14** to the enzyme is not as tight as that of **10**. Also, residue Gln167, one of the conserved residues in α-helix F, adopts a different conformation in the two complexes (Figure 4d.). The same is true about another conserved residue, Tyr211: in **14** its hydroxyl points away from bisphosphonate moiety. Interestingly, in the **14** complex Tyr211 points towards the isoprenyl chain of the bound IPP and, as a result, it affects the IPP conformation.

Inhibitor Affinities

Bisphosphonates derived from fatty acids have become interesting potential antiparasitic agents, especially 2-alkylaminoethyl derivatives, which were shown to be potent growth inhibitors of the most clinically relevant form of *T. cruzi* with IC_{50} values in the nanomolar range against the target enzyme[38, 41]. Compounds **10–14** are representative members of the 2-alkylaminoethyl family of bisphosphonates, which have proven to be far more efficient growth inhibitors of trypanosomatids than their parent drugs 1-hydroxy-, 1-alkyl-, and 1-amino-bisphosphonates such as compounds **7**, **8** and **9** (Figure 6).[39, 41, 42] Compounds **10–14** inhibit the enzymatic activity of *Tc*FPPS with IC_{50} values of 38 nM, 1.84 μM, 0.49 μM, 58 nM, 13 nM, respectively (Table 2).[40]

Thermodynamic Data

The interactions of *Tc*FPPS with these 2-alkylaminoethyl bisphosphonates were studied by isothermal titration calorimetry at 28 °C. (ITC data for *reversible* binding of **14** to TcFPPS could not be obtained.) The four compounds with *n*-alkyl chains, bind to the target enzyme with a positive, unfavorable enthalpy change (Figure 7; Table 2), in agreement with previous studies with other bisphosphonates[52]. This unfavorable enthalpy is compensated by large favorable entropy that is itself determined by the difference between to opposite effects. As the inhibitor molecules bind, the single bond rotations around the C—C bonds of the alkyl chain become frozen in the complex resulting in a loss of conformational entropy that becomes larger as the number of carbons in the alkyl chain increases. At the same time, the favorable entropy from the burial of the hydrophobic alkyl chain, also increases with chain length, resulting in a very fine balance between these two effects. The values of the unfavorable binding enthalpy also vary significantly among the inhibitors. **12** is the most unfavorable by 1.5–2.0 Kcal/mol.

The high affinity of **14** (IC_{50} 13 nM) can be rationalized based on these same arguments. TcFPPS binds **14** in a manner similar to **10**, suggesting that it would have a similar enthalpy of binding (not measured), although somewhat more unfavorable due to changes in the conformations of Gln167 and Tyr211 described above. However, **14** buries a large hydrophobic surface without the loss of conformational entropy of the *n*-alkyl chain experienced by the other inhibitors: the conformational flexibility of the ring is highly restricted even in the unbound state.

Furthermore, binding in the more stable chair conformation not only reduces the loss of entropy but also avoids the enthalpic penalty of binding the less favorable boat conformation.

The inhibition data (IC_{50}) of bisphosphonates **10–13** against TcFPPS are in excellent agreement with the K_d's obtained in the ITC experiments (Table 2). These results and the structural data taken together indicate that inhibition results from binding of these inhibitors to the allylic portion of the catalytic site of the enzyme. It is likely that other closely related bisphosphonates that effectively inhibit the enzymatic activity of TcFPPS also do so by binding to the allylic site.[41] The data for **13** can also be fit using two different sites per dimer (see figure 7 and Table 2 and their footnotes). This is similar to previous data on other nitrogen-containing bisphosphonates[52]. One reason for this behavior of **13** may be its size. Like some of the other large bisphosphonates, binding of **13** to one site of the dimer, modifies the affinity of the other monomer.

Towards the design of new bisphosphonate TcFPPS inhibitors

As mentioned above, binding of these inhibitors is enthalpically unfavorable. The favorable entropy, which dominates the favorable free-energy, results from a delicate balance two opposing effects: the unfavorable loss of conformational entropy, due to freezing of single bond rotations of the inhibitor (and binding site side chains), and the favorable increase of entropy associated with burial of the hydrophobic alkyl chains. With the shortest compound, *n*-propyl, the balance produces the tightest binding of the series. Increasing the length of the alkyl chain to pentyl or hexyl reduces the affinity by over an order of magnitude. This change seems to imply that by the addition of two or three methylenes, the increase in the loss of conformational entropy is greater than the additional entropy gain due to burial of the longer chain (more so for the pentyl than for the hexyl). This tendency is reversed when the *n*-alkyl chain is seven carbons long (**13** vs. **12**, Table 2). This observation suggests that increasing the alkyl chain further could generate compounds with higher affinity. However, analysis of the structure of the complex of TcFPPS with the *n*-heptyl inhibitor shows that increasing the *n*-alkyl chain past seven carbons would result in clashes with residues of the enzyme: in any of its possible positions the eighth carbon would clash with either Tyr94, His93, or Ile129 of chain B.

Comparison of the structure of the **13**-TcFPPS complex with the previously determined structure of the chicken FPPS (GgFPPS) in complex with GPP (geranyl pyrophosphate) provides crucial information for guiding the design of improved inhibitors: the N1 of **13** occupies the same position in the binding site as the C1 of the GPP (Figure 8) and the rest of the chains align up to the C6 of **13** that overlaps with C7 of the GPP. C7 of GPP is a tertiary carbon with two methyl groups while the equivalent carbon of **13** (C6) has only one methyl. The terminal methyl of **13** occupies a position between the positions occupied by the two GPP methyls, rendering this portion of **13** less complementary to the binding site. Adding a methyl group to the C6 of **13** is likely to result in a better inhibitor. The same is true of the C3 methyl of GPP: adding a methyl group at the C2 of **13** can fill this pocket. Furthermore, the bound conformation of **13** is compatible with the double bonds of GPP, suggesting that introducing double bonds at C1 and C5 of **13** will freeze the compound in the bound

conformation. This modification would reduce the loss of conformational entropy without affecting the binding enthalpy. The resulting compound with a 2,6-dimethyl-1,5-diene would be an excellent mimic of the bound GPP; however it would contain a labile enamine functionality that renders the compound too unstable to be considered a useful inhibitor. These observations point to a 2-alkylaminoethyl-1,1-bisphosphonate with an (*E*)-2-2,6-dimethylhepta-2,5-diene chain (compound **21**, Figure 9) as a highly promising lead compound for the next generation of bisphosphonate TcFPPS inhibitors (Figure 8b; Figure 9). Molecular modeling using MOE (Molecular Operating Environment, Chemical computing group; Quebec, Canada) showed that the 2,5 diene chain can bind the enzyme in a conformation that still mimics that of the bound geranyl diphosphate. It appears that the affinity of **10** can also be improved by an equivalent modification. Replacement of the propyl chain by an isobutyl-2-ene (compound **20**, Figure 9) would result in a compound that binds the enzyme mimicking DMAPP. In addition, the compounds equivalent to **20** and **21** but lacking the double bond at the 2-positions may also show high affinity for the enzyme.

EXPERIMENTAL SECTION

Synthesis of inhibitors

Compounds **10**–**14** were synthesized as reported before[40]. In brief; they were prepared using tetraethyl ethenylidene bisphosphonate (compound **15**) as a Michael acceptor,[53] which in turn was prepared from tetraethyl methylenebisphosphonate in two steps according to a slightly modified Degenhart protocol.[54] Compound **15** was reacted with the corresponding *n*-alkylamine *via* a 1,4-conjugated addition reaction to yield the respective Michael adducts (**16**–**20**). Once these synthetic precursors were at hand, they were hydrolyzed with bromotrimethylsilane in methylene chloride[55] to afford the free 1,1-bisphosphonic acids (**10**–**14**).[39] The purity of the compounds assessed by elemental analysis was greater than 98%[40].

Cloning, expression and purification

TcFPPS was cloned and expressed as reported before[56]. Briefly, DNA coding for TcFPPS with an N-terminal His-Tag and a thrombin cleaveage site was cloned into a pET28a vector (Novagen). BL21(DE3) *E. coli* cells transformed with this plasmid were grown in LB medium until they reached an OD_{600} of 0.8 and induced with 0.1 mM IPTG at 37.0 °C. The cells were harvested 3h after induction, washed in buffer A (50 mM NaH_2PO_4 pH 8.0 300 mM NaCl, 10 mM imidazole, 1 mM TCEP; TCEP: tris(2-carboxyethyl) phosphine hydrochloride), and broken with a microfluidizer. The lysate was centrifuged for 30 mins at 12000 rpm and the supernatant was loaded onto a HisTrap Ni^{2+} chelate affinity column equilibrated with buffer A. The protein was eluted using a linear gradient of 0–100% of buffer B (50 mM NaH_2PO_4 pH 8.0 300 mM NaCl, 500 mM Imidazole, 1 mM TCEP). The His-tag was cleaved by digestion with thrombin and the sample was loaded into an anion exchange column (binding buffer: 20 mM Tris pH 8.2, 20 mM NaCl, 1 mM TCEP) and eluted with 20 mM Tris pH 8.2, 1 M NaCl, 1 mM TCEP. The protein, which was more than 95% pure as seen by SDS page gel, was dialyzed against 20 mM Tris pH 8.2, 150 mM NaCl, 1 mM TCEP and concentrated to 12 mg mL^{-1}.

Crystallization

Crystals used for data collection were grown by vapor diffusion with the protein and the mother liquor in a 1:1 ratio. The reservoir consisted of 100 mM sodium acetate, pH 4.6–5.2, 200 mM ammonium sulfate, and 2–10% PEG 4K. Crystals, which appear within 1–2 days, belong to the hexagonal space group $P6_122$. The protein (12.5 mg/ml) inhibitor solution used for co-crystallization contained 250 μM inhibitor, 250 μM IPP and 1 mM $MgCl_2$.

Data Collection

Diffraction data of all the TcFPPS complexes were collected at beamline X6A of the NSLS, Brookhaven National Laboratory. Diffraction data collected from a single frozen crystal (100 K) were processed and scaled using the HKL 2000 suite[57] (Table 1).

Structure Determination

The structures of the complexes of TcFPPS with compounds **11–14** were determined by direct refinement of the coordinates of the FPPS from Trypanosoma cruzi (1YHM)[48] with the program REFMAC5[58–60] of CCP4 suite. The structure of **10** was determined by molecular replacement using the program AMoRe[61] (search molecule PDB id 1YHM).

Model Building and Refinement

The initial model was refined using REFMAC5 and rebuilding during refinement was carried out with the program COOT[62]. Following the R-value monitored progress of the refinement and an R-free calculated with a cross validation set containing 5% of the reflections. The overall quality of the final model was assessed using the programs PROCHECK[63] and WHATIF[64, 65]. Atomic coordinates and structure factors for the complexes TcFPPS+**10**, TcFPPS+**11**, TcFPPS+**12**, TcFPPS+**13** and TcFPPS+**14** have been deposited in the Protein Data Bank with accession codes 4DWB, 4DXJ, 4DWG, 4EIE and 4DZW respectively. Structure figures were generated using molscript[66] and pymol (The PyMOL Molecular Graphics System, Version 1.5.0.1 Schrödinger, LLC). Models of the proposed new inhibitors were built using MOE (Molecular Operating Environment, Quebec, Canada).

Isothermal Calorimetry

ITC experiments were performed with TcFPPS and each of five ligands: **10–14**. The protein was diluted to a concentration of 29 μM (in monomers) in a buffer containing 25 mM Hepes pH 7.5, 1 mM TCEP, 300 mM NaCl, 2 mM $MgCl_2$. The ligands were prepared in the same buffer at a concentration of 250 μM. 1.3 mL of protein in the sample cell were titrated with twenty five 10 μl injections. The data were analyzed with the Origin-5.0 software and fitted to a single binding site per monomer.

Acknowledgments

This work was supported by grants from the National Research Council of Argentina (PIP 1888), ANPCyT (PICT 2008 #1690), and the Universidad de Buenos Aires (20020100100380l) to J.B.R and Bunge & Born Foundation to S.H.S. Data collection was carried out at beam line X6A, funded by the National Institute of General Medical Sciences, National Institute of Health under agreement GM-0080. The NSLS, Brookhaven National Laboratory is supported by the US Department of energy under contract No. DE AC02-98CH10886.

Abbreviations

FPPS	Farnesyl pyrophosphate synthase
FPP	Farnesyl pyrophosphate
GPP	Geranyl pyrophosphate
BPs	Bisphosphonates
TcFPPS	*Trypanosoma cruzi* Farnesyl pyrophosphate synthase
IPP	Isopentanyl pyrophosphate
DMAPP	Dimethylallyl pyrophosphate

References

1. Urbina JA, Docampo R. Specific chemotherapy of Chagas disease: controversies and advances. Trends Parasitol. 2003; 19:495–501. [PubMed: 14580960]
2. WHO. http://www.who.int/topics/tropical_diseases/en/
3. Brener Z. Biology of Trypanosoma cruzi. Annu Rev Microbiol. 1973; 27:347–382. [PubMed: 4201691]
4. Kirchhoff LV. American trypanosomiasis (Chagas' disease)--a tropical disease now in the United States. N Engl J Med. 1993; 329:639–644. [PubMed: 8341339]
5. Galel SA, Kirchhoff LV. Risk factors for Trypanosoma cruzi infection in California blood donors. Transfusion. 1996; 36:227–231. [PubMed: 8604507]
6. Urbina JA. Specific chemotherapy of Chagas disease: relevance, current limitations and new approaches. Acta Trop. 2010; 115:55–68. [PubMed: 19900395]
7. Roelofs AJ, Thompson K, Ebetino FH, Rogers MJ, Coxon FP. Bisphosphonates: molecular mechanisms of action and effects on bone cells, monocytes and macrophages. Curr Pharm Des. 2010; 16:2950–2960. [PubMed: 20722616]
8. Reszka AA, Rodan GA. Nitrogen-containing bisphosphonate mechanism of action. Mini Rev Med Chem. 2004; 4:711–719. [PubMed: 15379639]
9. Russell RG, Rogers MJ. Bisphosphonates: from the laboratory to the clinic and back again. Bone. 1999; 25:97–106. [PubMed: 10423031]
10. Reszka AA, Rodan GA. Mechanism of action of bisphosphonates. Curr Osteoporos Rep. 2003; 1:45–52. [PubMed: 16036064]
11. Fleisch H, Russell RG, Straumann F. Effect of pyrophosphate on hydroxyapatite and its implications in calcium homeostasis. Nature. 1966; 212:901–903. [PubMed: 4306793]
12. Fleisch H, Russell RG, Francis MD. Diphosphonates inhibit hydroxyapatite dissolution in vitro and bone resorption in tissue culture and in vivo. Science. 1969; 165:1262–1264. [PubMed: 5803538]
13. Francis MD, Russell RG, Fleisch H. Diphosphonates inhibit formation of calcium phosphate crystals in vitro and pathological calcification in vivo. Science. 1969; 165:1264–1266. [PubMed: 4308521]
14. Urbina JA, Moreno B, Vierkotter S, Oldfield E, Payares G, Sanoja C, Bailey BN, Yan W, Scott DA, Moreno SN, Docampo R. Trypanosoma cruzi contains major pyrophosphate stores, and its growth in vitro and in vivo is blocked by pyrophosphate analogs. J Biol Chem. 1999; 274:33609–33615. [PubMed: 10559249]
15. Hughes DE, Wright KR, Uy HL, Sasaki A, Yoneda T, Roodman GD, Mundy GR, Boyce BF. Bisphosphonates promote apoptosis in murine osteoclasts in vitro and in vivo. J Bone Miner Res. 1995; 10:1478–1487. [PubMed: 8686503]
16. Rogers MJ, Frith JC, Luckman SP, Coxon FP, Benford HL, Monkkonen J, Auriola S, Chilton KM, Russell RG. Molecular mechanisms of action of bisphosphonates. Bone. 1999; 24:73S–79S. [PubMed: 10321934]

17. Kavanagh KL, Guo K, Dunford JE, Wu X, Knapp S, Ebetino FH, Rogers MJ, Russell RG, Oppermann U. The molecular mechanism of nitrogen-containing bisphosphonates as antiosteoporosis drugs. Proc Natl Acad Sci U S A. 2006; 103:7829–7834. [PubMed: 16684881]
18. Hosfield DJ, Zhang Y, Dougan DR, Broun A, Tari LW, Swanson RV, Finn J. Structural basis for bisphosphonate-mediated inhibition of isoprenoid biosynthesis. J Biol Chem. 2004; 279:8526–8529. [PubMed: 14672944]
19. Rondeau JM, Bitsch F, Bourgier E, Geiser M, Hemmig R, Kroemer M, Lehmann S, Ramage P, Rieffel S, Strauss A, Green JR, Jahnke W. Structural basis for the exceptional in vivo efficacy of bisphosphonate drugs. Chem Med Chem. 2006; 1:267–273. [PubMed: 16892359]
20. Cheng F, Oldfield E. Inhibition of isoprene biosynthesis pathway enzymes by phosphonates, bisphosphonates, and diphosphates. J Med Chem. 2004; 47:5149–5158. [PubMed: 15456258]
21. Dunford JE, Thompson K, Coxon FP, Luckman SP, Hahn FM, Poulter CD, Ebetino FH, Rogers MJ. Structure-activity relationships for inhibition of farnesyl diphosphate synthase in vitro and inhibition of bone resorption in vivo by nitrogen-containing bisphosphonates. J Pharmacol Exp Ther. 2001; 296:235–242. [PubMed: 11160603]
22. van Beek E, Pieterman E, Cohen L, Lowik C, Papapoulos S. Farnesyl pyrophosphate synthase is the molecular target of nitrogen-containing bisphosphonates. Biochem Biophys Res Commun. 1999; 264:108–111. [PubMed: 10527849]
23. Coxon FP, Thompson K, Rogers MJ. Recent advances in understanding the mechanism of action of bisphosphonates. Curr Opin Pharmacol. 2006; 6:307–312. [PubMed: 16650801]
24. Sanders JM, Ghosh S, Chan JM, Meints G, Wang H, Raker AM, Song Y, Colantino A, Burzynska A, Kafarski P, Morita CT, Oldfield E. Quantitative structure-activity relationships for gammadelta T cell activation by bisphosphonates. J Med Chem. 2004; 47:375–384. [PubMed: 14711309]
25. Reddy R, Dietrich E, Lafontaine Y, Houghton TJ, Belanger O, Dubois A, Arhin FF, Sarmiento I, Fadhil I, Laquerre K, Ostiguy V, Lehoux D, Moeck G, Parr TR Jr, Rafai Far A. Bisphosphonated benzoxazinorifamycin prodrugs for the prevention and treatment of osteomyelitis. Chem Med Chem. 2008; 3:1863–1868. [PubMed: 18973169]
26. Forlani G, Giberti S, Berlicki L, Petrollino D, Kafarski P. Plant P5C reductase as a new target for aminomethylenebisphosphonates. J Agric Food Chem. 2007; 55:4340–4347. [PubMed: 17474756]
27. Clezardin P, Massaia M. Nitrogen-containing bisphosphonates and cancer immunotherapy. Curr Pharm Des. 2010; 16:3007–2014. [PubMed: 20722623]
28. Miller K, Erez R, Segal E, Shabat D, Satchi-Fainaro R. Targeting bone metastases with a bispecific anticancer and antiangiogenic polymer-alendronate-taxane conjugate. Angew Chem Int Ed Engl. 2009; 48:2949–2954. [PubMed: 19294707]
29. Zhang Y, Cao R, Yin F, Hudock MP, Guo RT, Krysiak K, Mukherjee S, Gao YG, Robinson H, Song Y, No JH, Bergan K, Leon A, Cass L, Goddard A, Chang TK, Lin FY, Van Beek E, Papapoulos S, Wang AH, Kubo T, Ochi M, Mukkamala D, Oldfield E. Lipophilic bisphosphonates as dual farnesyl/geranylgeranyl diphosphate synthase inhibitors: an X-ray and NMR investigation. J Am Chem Soc. 2009; 131:5153–5162. [PubMed: 19309137]
30. Coleman RE. Risks and benefits of bisphosphonates. Br J Cancer. 2008; 98:1736–1740. [PubMed: 18506174]
31. Docampo R, Moreno SN. The acidocalcisome as a target for chemotherapeutic agents in protozoan parasites. Curr Pharm Des. 2008; 14:882–888. [PubMed: 18473837]
32. Oldfield E. Targeting isoprenoid biosynthesis for drug discovery: bench to bedside. Acc Chem Res. 2010; 43:1216–1226. [PubMed: 20560544]
33. Ghosh S, Chan JM, Lea CR, Meints GA, Lewis JC, Tovian ZS, Flessner RM, Loftus TC, Bruchhaus I, Kendrick H, Croft SL, Kemp RG, Kobayashi S, Nozaki T, Oldfield E. Effects of bisphosphonates on the growth of Entamoeba histolytica and Plasmodium species in vitro and in vivo. J Med Chem. 2004; 47:175–187. [PubMed: 14695831]
34. Martin MB, Grimley JS, Lewis JC, Heath HT 3rd, Bailey BN, Kendrick H, Yardley V, Caldera A, Lira R, Urbina JA, Moreno SN, Docampo R, Croft SL, Oldfield E. Bisphosphonates inhibit the growth of Trypanosoma brucei, Trypanosoma cruzi, Leishmania donovani, Toxoplasma gondii, and Plasmodium falciparum: a potential route to chemotherapy. J Med Chem. 2001; 44:909–916. [PubMed: 11300872]

35. Yardley V, Khan AA, Martin MB, Slifer TR, Araujo FG, Moreno SN, Docampo R, Croft SL, Oldfield E. In vivo activities of farnesyl pyrophosphate synthase inhibitors against Leishmania donovani and Toxoplasma gondii. Antimicrob Agents Chemother. 2002; 46:929–931. [PubMed: 11850291]

36. Bouzahzah B, Jelicks LA, Morris SA, Weiss LM, Tanowitz HB. Risedronate in the treatment of Murine Chagas' disease. Parasitol Res. 2005; 96:184–187. [PubMed: 15844009]

37. Martin MB, Sanders JM, Kendrick H, de Luca-Fradley K, Lewis JC, Grimley JS, Van Brussel EM, Olsen JR, Meints GA, Burzynska A, Kafarski P, Croft SL, Oldfield E. Activity of bisphosphonates against Trypanosoma brucei rhodesiense. J Med Chem. 2002; 45:2904–2914. [PubMed: 12086478]

38. Rosso VS, Szajnman SH, Malayil L, Galizzi M, Moreno SN, Docampo R, Rodriguez JB. Synthesis and biological evaluation of new 2-alkylaminoethyl-1,1-bisphosphonic acids against Trypanosoma cruzi and Toxoplasma gondii targeting farnesyl diphosphate synthase. Bioorg Med Chem. 2011; 19:2211–2217. [PubMed: 21419634]

39. Szajnman SH, Bailey BN, Docampo R, Rodriguez JB. Bisphosphonates derived from fatty acids are potent growth inhibitors of Trypanosoma cruzi. Bioorg Med Chem Lett. 2001; 11:789–792. [PubMed: 11277521]

40. Szajnman SH, Garcia Linares GE, Li ZH, Jiang C, Galizzi M, Bontempi EJ, Ferella M, Moreno SN, Docampo R, Rodriguez JB. Synthesis and biological evaluation of 2-alkylaminoethyl-1,1-bisphosphonic acids against Trypanosoma cruzi and Toxoplasma gondii targeting farnesyl diphosphate synthase. Bioorg Med Chem. 2008; 16:3283–3290. [PubMed: 18096393]

41. Szajnman SH, Montalvetti A, Wang Y, Docampo R, Rodriguez JB. Bisphosphonates derived from fatty acids are potent inhibitors of Trypanosoma cruzi farnesyl pyrophosphate synthase. Bioorg Med Chem Lett. 2003; 13:3231–3235. [PubMed: 12951099]

42. Szajnman SH, Ravaschino EL, Docampo R, Rodriguez JB. Synthesis and biological evaluation of 1-amino-1,1-bisphosphonates derived from fatty acids against Trypanosoma cruzi targeting farnesyl pyrophosphate synthase. Bioorg Med Chem Lett. 2005; 15:4685–4690. [PubMed: 16143525]

43. Ling Y, Sahota G, Odeh S, Chan JM, Araujo FG, Moreno SN, Oldfield E. Bisphosphonate inhibitors of Toxoplasma gondi growth: in vitro, QSAR, and in vivo investigations. J Med Chem. 2005; 48:3130–3140. [PubMed: 15857119]

44. Laskovics FM, Krafcik JM, Poulter CD. Prenyltransferase. Kinetic studies of the 1′-4 coupling reaction with avian liver enzyme. J Biol Chem. 1979; 254:9458–9463. [PubMed: 489545]

45. Laskovics FM, Poulter CD. Prenyltransferase; determination of the binding mechanism and individual kinetic constants for farnesylpyrophosphate synthetase by rapid quench and isotope partitioning experiments. Biochemistry. 1981; 20:1893–1901. [PubMed: 7013805]

46. Poulter CD, Argyle JC, Mash EA. Farnesyl pyrophosphate synthetase. Mechanistic studies of the 1′-4 coupling reaction with 2-fluorogeranyl pyrophosphate. J Biol Chem. 1978; 253:7227–7233. [PubMed: 701246]

47. Ding VD, Sheares BT, Bergstrom JD, Ponpipom MM, Perez LB, Poulter CD. Purification and characterization of recombinant human farnesyl diphosphate synthase expressed in Escherichia coli. Biochem J. 1991; 275(Pt 1):61–65. [PubMed: 2018485]

48. Gabelli SB, McLellan JS, Montalvetti A, Oldfield E, Docampo R, Amzel LM. Structure and mechanism of the farnesyl diphosphate synthase from Trypanosoma cruzi: implications for drug design. Proteins. 2006; 62:80–88. [PubMed: 16288456]

49. Ohnuma S, Nakazawa T, Hemmi H, Hallberg AM, Koyama T, Ogura K, Nishino T. Conversion from farnesyl diphosphate synthase to geranylgeranyl diphosphate synthase by random chemical mutagenesis. J Biol Chem. 1996; 271:10087–10095. [PubMed: 8626566]

50. Tarshis LC, Proteau PJ, Kellogg BA, Sacchettini JC, Poulter CD. Regulation of product chain length by isoprenyl diphosphate synthases. Proc Natl Acad Sci U S A. 1996; 93:15018–15023. [PubMed: 8986756]

51. Narita K, Ohnuma S, Nishino T. Protein design of geranyl diphosphate synthase. Structural features that define the product specificities of prenyltransferases J Biochem. 1999; 126:566–571. [PubMed: 10467173]

52. Huang CH, Gabelli SB, Oldfield E, Amzel LM. Binding of nitrogen-containing bisphosphonates (N-BPs) to the Trypanosoma cruzi farnesyl diphosphate synthase homodimer. Proteins. 2010; 78:888–899. [PubMed: 19876942]

53. Szajnman SH, Linares GG, Moro P, Rodriguez JB. New insights into the chemistry of gem-bis(phosphonates): Unexpected rearrangement of Michael-type acceptors. European Journal of Organic Chemistry. 2005:3687–3696.

54. Degenhardt CR, Burdsall DC. Synthesis of Ethenylidenebis(Phosphonic Acid) and Its Tetraalkyl Esters. Journal of Organic Chemistry. 1986; 51:3488–3490.

55. Lazzarato L, Rolando B, Lolli ML, Tron GC, Fruttero R, Gasco A, Deleide G, Guenther HL. Synthesis of NO-donor bisphosphonates and their in-vitro action on bone resorption. J Med Chem. 2005; 48:1322–1329. [PubMed: 15743175]

56. Huang CH, Gabelli SB, Oldfield E, Amzel LM. Binding of nitrogen-containing bisphosphonates (N-BPs) to the Trypanosoma cruzi farnesyl diphosphate synthase homodimer. Proteins. 78:888–899. [PubMed: 19876942]

57. Otwinowski Z, Minor W. Processing of X-ray diffraction data collected in oscillation mode. Macromolecular Crystallography, Pt A. 1997; 276:307–326.

58. Winn MD, Isupov MN, Murshudov GN. Use of TLS parameters to model anisotropic displacements in macromolecular refinement. Acta Crystallographica Section D-Biological Crystallography. 2001; 57:122–133.

59. Murshudov GN, Skubak P, Lebedev AA, Pannu NS, Steiner RA, Nicholls RA, Winn MD, Long F, Vagin AA. REFMAC5 for the refinement of macromolecular crystal structures. Acta Crystallographica Section D-Biological Crystallography. 2011; 67:355–367.

60. Bailey S. The Ccp4 Suite - Programs for Protein Crystallography. Acta Crystallographica Section D-Biological Crystallography. 1994; 50:760–763.

61. Navaza J. Amore - an Automated Package for Molecular Replacement. Acta Crystallographica Section A. 1994; 50:157–163.

62. Emsley P, Lohkamp B, Scott WG, Cowtan K. Features and development of Coot. Acta Crystallographica Section D-Biological Crystallography. 2010; 66:486–501.

63. Laskowski RA, Macarthur MW, Moss DS, Thornton JM. Procheck - a Program to Check the Stereochemical Quality of Protein Structures. Journal of Applied Crystallography. 1993; 26:283–291.

64. Hooft RW, Vriend G, Sander C, Abola EE. Errors in protein structures. Nature. 1996; 381:272. [PubMed: 8692262]

65. Hooft RWW, Sander C, Vriend G. Verification of protein structures: Side-chain planarity. Journal of Applied Crystallography. 1996; 29:714–716.

66. Kraulis PJ. Molscript - a Program to Produce Both Detailed and Schematic Plots of Protein Structures. Journal of Applied Crystallography. 1991; 24:946–950.

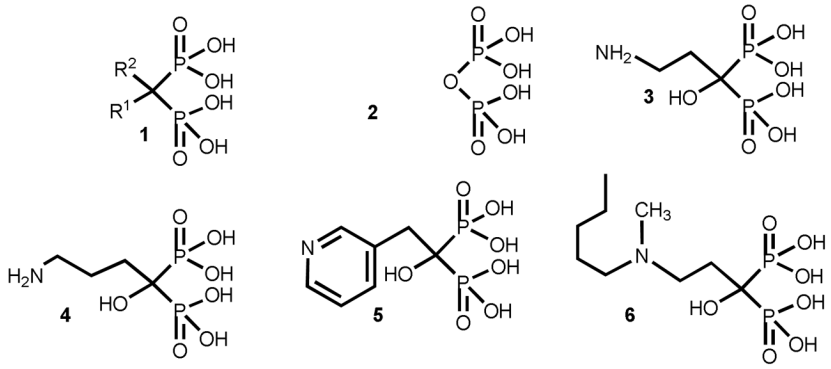

Figure 1.

General formula and chemical structure of pyrophosphate and bisphosphonates. 1-general bisphosphonate; 2-pyrophosphate; 3–6-representative FDA-approved bisphosphonates clinically employed for different bone disorders: 3, palmidronate; 4, alendronate; 5, residronate; 6, ibandronate.

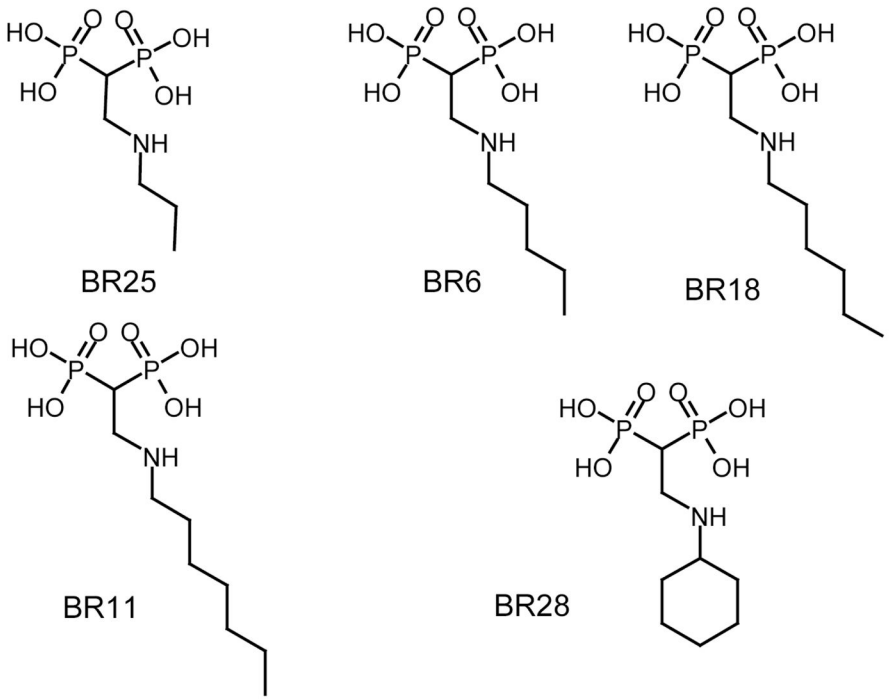

Figure 2.

Bisphosphonate drugs used in this study[40]. [2-(n-propylamino)ethane-1,1-diyl]bisphosphonic acid (BR25 = **10**); [2-(n-pentylamino)ethane-1,1-diyl]bisphosphonic acid (BR6 = **11**); [2-(n-hexylamino) ethane-1,1-diyl]bisphosphonic acid (BR18 = **12**); [2-(n-heptylamino)ethane-1,1-diyl]bisphosphonic acid (BR11 = **13**[38, 40, 42]); [2-(cyclohexylamino)ethane-1,1-diyl]bisphosphonic acid (BR28 = **14**).

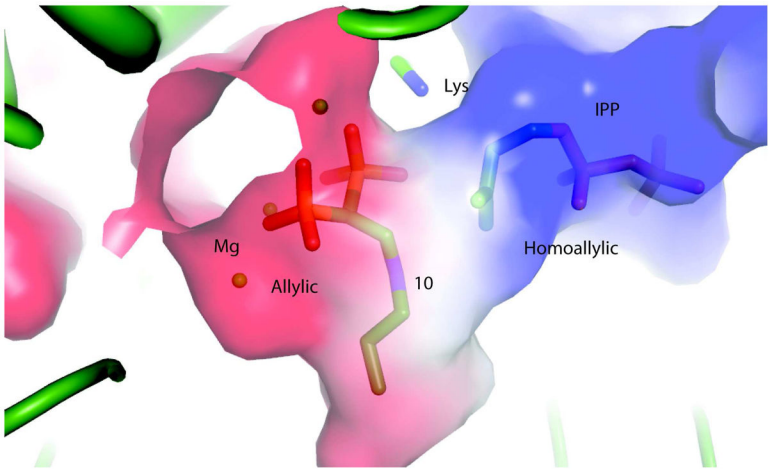

Figure 3.

Allylic and homoallylic sites of FPPS. The allylic site is the part of the active site occupied by Mg and the bisphosphonate **10**. The Homoallylic site is occupied by IPP. Magnesiums are shown in cpk model while the ligands **10** and IPP are shown as a stick model. The surface shows positive potential as blue and negative as red.

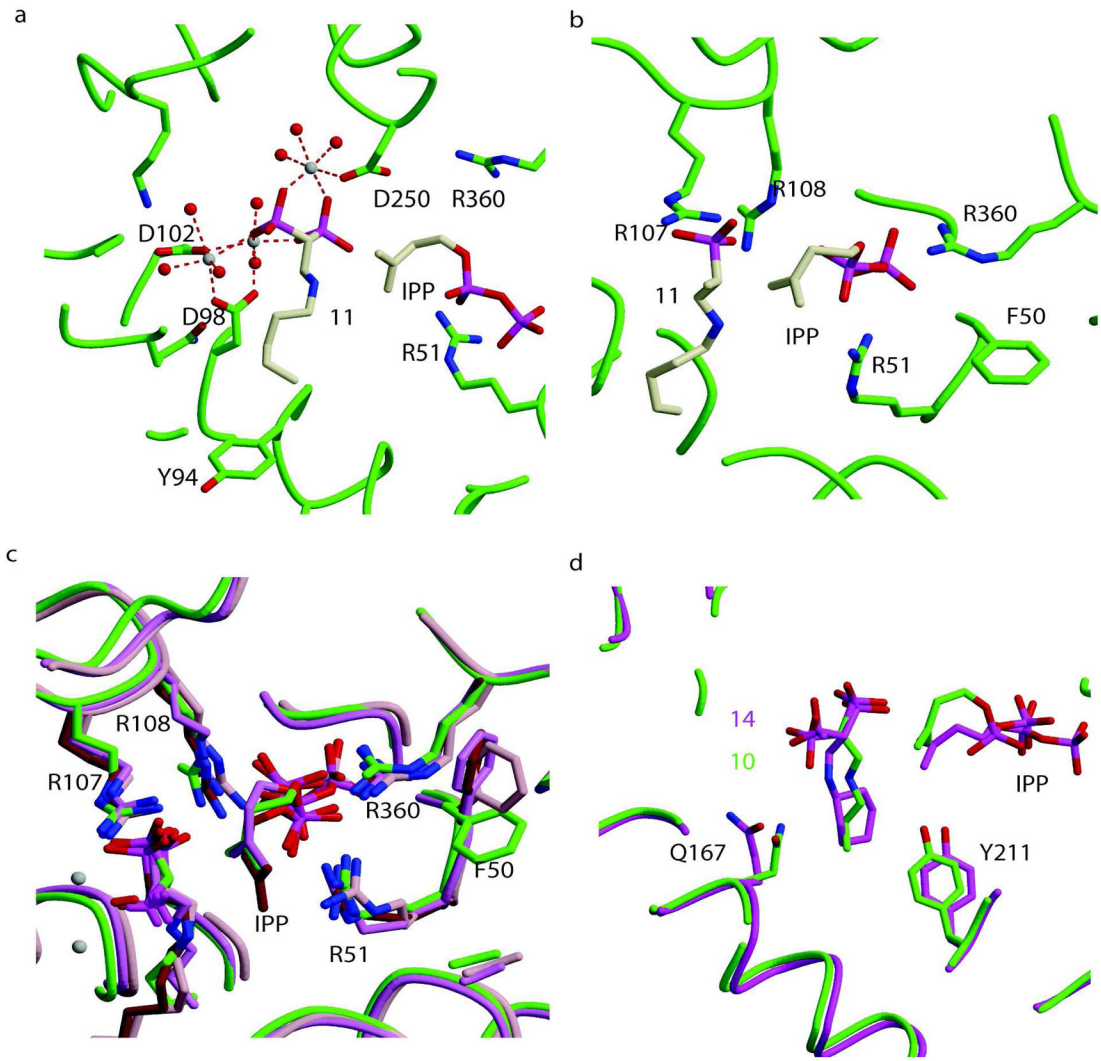

Figure 4.

Binding of bisphosphonates in various complexes of TcFPPS. (a) TcFPPS in complex with **11**, IPP and 3 divalent cations. Water molecules are shown as red spheres and Mg^{2+} in white. Protein backbone and residues of the active site are shown in green color. **11** and IPP are shown in cream color. Residues from the FARM and SARM are shown coordinating with Mg^{2+} ions. The basic amino acids Arg360 and Arg51 are observed to be interacting with the diphosphate moiety of IPP. (b) Homoallylic site of TcFPPS in complex with **11** (cream) and IPP (cream). IPP interacts with the basic amino acids Arg51 and Arg360. Arg107 and Arg108, from the loop after first aspartate rich region, interact with the inhibitor in the allylic site (**11**). (c) Structural overlap of the four BPs with *n*-alkyl chains (**10–13**) in complex with TcFPPS + Mg^{2+} + IPP (green). (d) Structural overlap of TcFPPS in complex with **10** (green) and with **14** (magenta). Residues in the TcFPPS-**10** complex are shown in green color and those of TcFPPS-**14** complex in magenta. Key differences in the conserved interactions of the ligands with residues of the active site are shown.

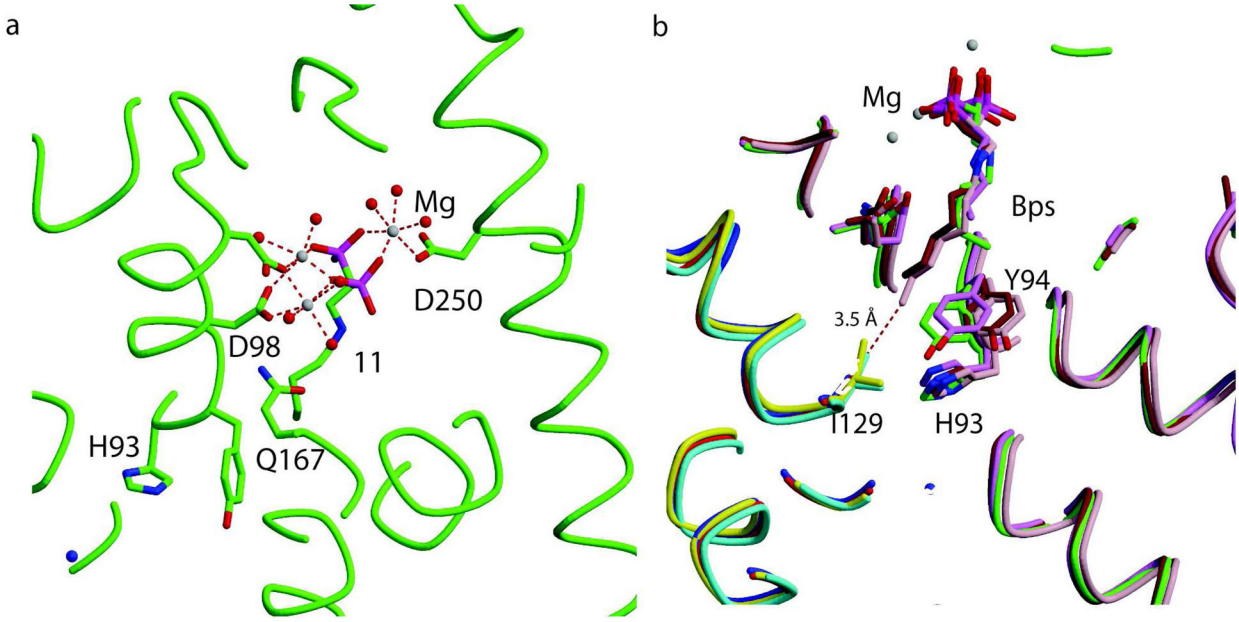

Figure 5.

Allylic site binding of inhibitors in various TcFPPS-BPs complexes. (a) TcFPPS in complex with **11** and 3 divalent cations. Water molecules are shown as red spheres, Mg^{2+} in white. The TcFPPS protein backbone and some residues in the active site are shown in green color. **11** is shown as a stick model in green color. Residues from the first and second aspartate rich regions are shown coordinating the Mg^{2+} ions. (b) Structural overlap of TcFPPS in complex with four *n*-alkyl chain bisphosphonates **10–13**. Residues His93, Tyr94, Ile129 (monomer B) at the "bottom" of the allylic site are shown. Monomer A of the TcFPPS-**11** complex is shown in green, the TcFPPS-**13** complex in pink, TcFPPS-**12** complex in brown, TcFPPS-**10** complex in violet while monomer B is shown in red, cyan, yellow and blue respectively. The distance between the terminal carbon of the longest bisphosphonate **13** and the Ile 129 is 3.5 Å.

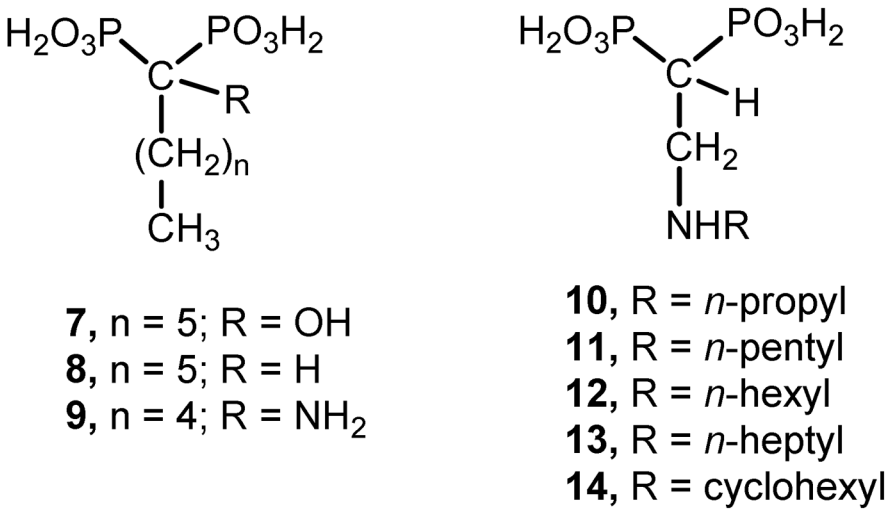

Figure 6.
Chemical structure of representative bisphosphonic acids derivatives.

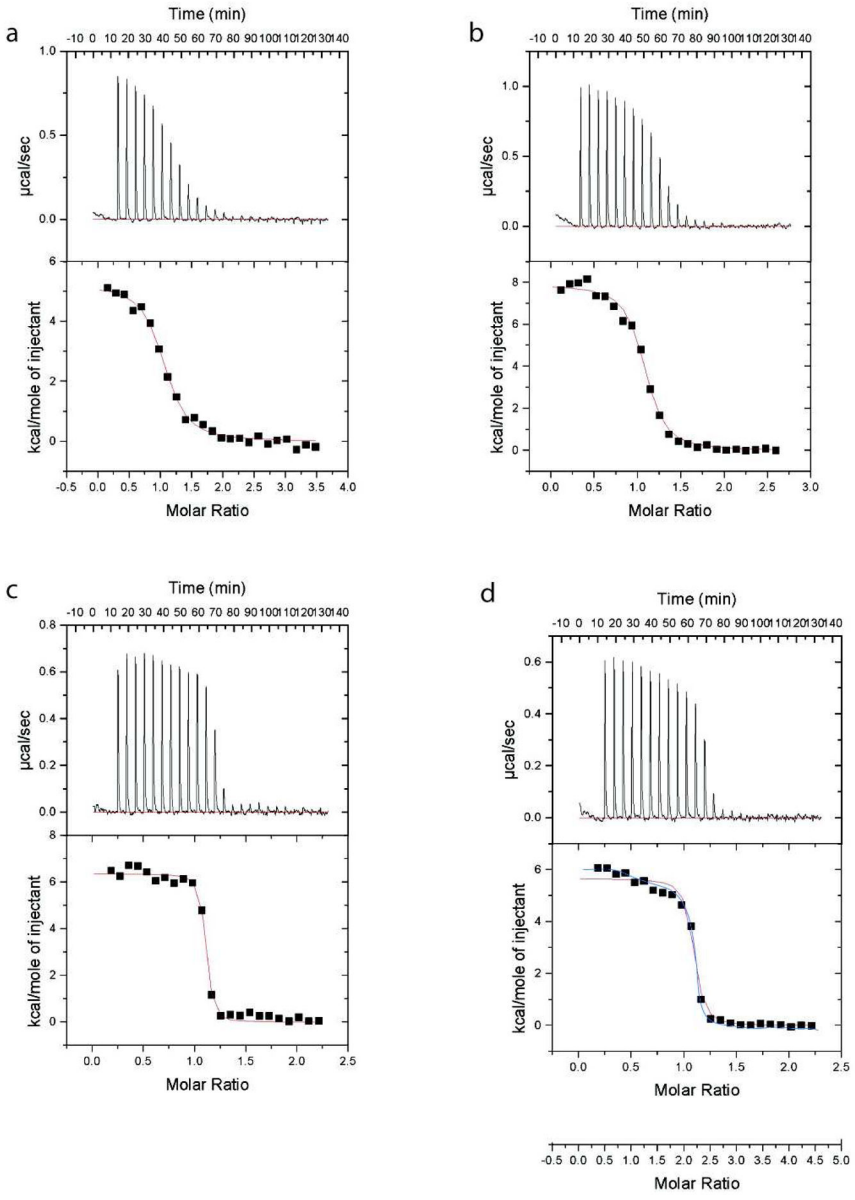

Figure 7.

Isothermal titration calorimetry of the reaction between bisphosphonate drugs and TcFPPS. (a) **11**. (b) **12**. (c) **10**. (d) **13. 13** can be fit either as two identical sites (one per monomer; red) or as two different sites (two per dimer; blue).

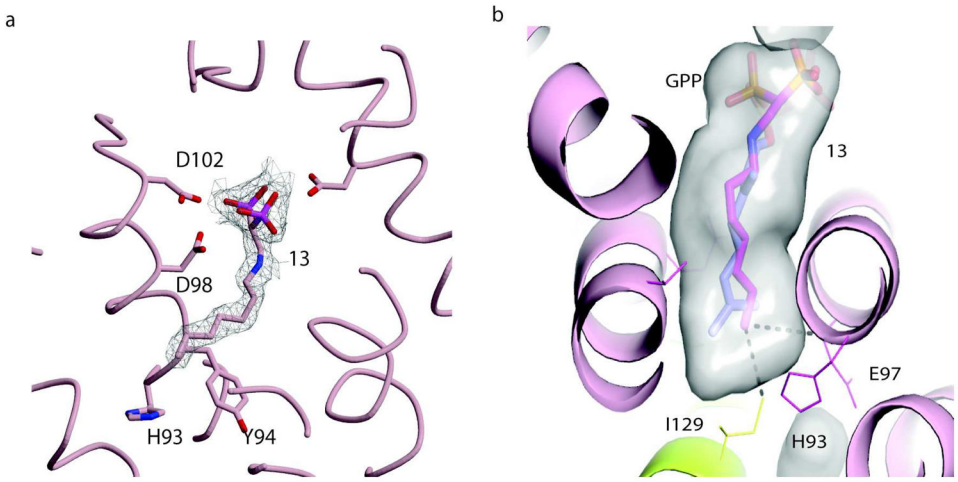

Figure 8.

Overlap of GPP and **13**. a) Allylic site of **13**-TcFPPS complex. **13**, amino acids are shown in stick representation (pink). Portion of the $2mF_o$-DF_c electron density corresponding to the inhibitor **13** is shown in grey color. b) Structural overlap of **13**-TcFPPS complex with the chicken FPPS-GPP complex (PDB: 1UBW). TcFPPS is shown in ribbon model (green). The ligands **13** (pink) and GPP (blue) in stick representation. Only GPP of the chicken FPPS is shown in the figure.

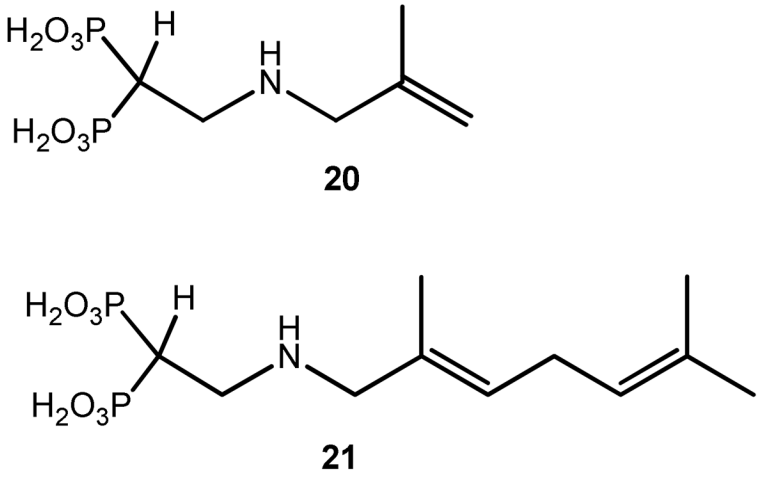

Figure 9.
New proposed bisphosphonates. Compounds labeled as **20** and **21**.

Table 1

Structures of TcFPPS complex: Data collection and Refinement Statistics

Crystal	**TcFPPS+IPP 11 + Mg^{2+}**	**TcFPPS+ 13 + Mg^{2+}**	**TcFPPS+IPP 12 + Mg^{2+}**	**TcFPPS+IPP 14 + Mg^{2+}**	**TcFPPS+IPP 10 + Mg^{2+}**
Space group	$P6_122$				
Cell dimensions(Å)	a = 57.9; b = 57.9; c = 392.4				a = 103.2
					b = 103.2
					c = 386.6
X-ray Source	BNL-X6a	BNL-X6a	BNL-X6a	BNL-X6a	BNL-X6a
Res(Å) (HighRes shell)	50.0-2.1	50.0-2.01	50.0-2.65	50.0-3.05	50.0-2.35
	(2.14-2.1)	(2.04-2.01)	(2.70-2.65)	(3.1-3.05)	(2.39-2.35)
Measured Reflect.	173,165	152,558	174,663	79,815	453,674
Unique Reflections	22,705	27,252	12,287	7,407	49,874
I/σ	23.6 (4.3)	34.3 (6.2)	38.0 (7.8)	46.9 (16.8)	26.6 (2.2)
Completeness (%)	93.2 (98.2)	97.8 (98.7)	95.7 (99.8)	87.8 (90.3)	96.0 (93.7)
R_{merge} (%)	11.3 (50.9)	8.0 (34.6)	10.5 (47.3)	6.9 (14.3)	9.0 (52.0)
Refinement					
R_{cryst} (%)	22.1	20.3	23.6	23.1	22.0
R_{free}	28.4	26.7	30.7	29.6	28.5
Monomer in ASU	1	1	1	1	3
Total Atoms	3,037	3,205	2,960	2,916	9,014
Protein atoms	2,900	2,900	2902	2854	8701
Water molecules	89	256	23	3	161
R.m.s deviations					
Bond length (Å)	0.021	0.02	0.008	0.007	0.009
Angle (°)	1.82	1.83	1.13	0.97	1.21
Bfactor($Å^2$)					
Protein	31.14	28.33	51.53	46.81	33.36
Allylic	36.23	27.25	40.18	47.54	29.54

Crystal	TcFPPS+IPP 11 + Mg^{2+}	TcFPPS+ 13 + Mg^{2+}	TcFPPS+IPP 12 + Mg^{2+}	TcFPPS+IPP 14 + Mg^{2+}	TcFPPS+IPP 10 + Mg^{2+}
Homoallylic	58.19	59.30	51.17	49.13*	44.72
H_20	35.01	35.59	34.12	26.10	30.51

* Occupancy: 0.6

Table 2

Isothermal Titration Calorimetry Studies on the Binding of Bisphosphonates to *Tc*FPPS

Lig	Carbons in *N*-alkyl	ΔG (kcal/mol)	ΔH (kcal/mol)	ΔS (cal/mol/K)	1/Ka (nM)	IC^{*}_{50} (nM)
10	3	−10.43	6.35 ± 0.07	56.1	25.0 ± 6.3	38.0
11	5	−8.15	5.22 ± 0.11	44.7	1030 ±170	1840
12	6	−8.72	7.87 ± 0.11	55.4	400 ± 63	490
13	7	−9.88	5.65 ± 0.09 † (6.39 ± 0.36; 4.62 ± 0.44)	51.9	58.8 ± 20.4 † (10.2 ± 7.3; 38.3 ± 11.2)	58.0

* IC50 were calculated before[40]

† Values calculated using 2-site model.